Heliyon 9 (2023) e12740

Contents lists available at ScienceDirect

Heliyon

journal homepage: www.cell.com/heliyon

Research article

Passivity-based boundary control with the backstepping observer for the vibration suppression of the flexible beam

Nipon Boonkumkrong [a,*], Sinchai Chinvorarat [b], Pichai Asadamongkon [a]

[a] Department of Mechanical Engineering, Faculty of Engineering, Srinakharinwirot University, Nakornnayok, 26120, Thailand
[b] Department of Mechanical and Aerospace Engineering, Faculty of Engineering, King Mongkut's University of Technology North Bangkok, Bangkok, 10800, Thailand

ARTICLE INFO

Keywords:
Passivity-based boundary control
Shear beam
Storage function
Backstepping observer
Vibration suppression
Partial differential equation

ABSTRACT

In engineering applications, flexible beam vibration control is an important issue. Although several researchers have discussed controlling beam vibration, there are few strategies for implementing it in actual applications. The passivity-based boundary control for suppressing flexible beam vibration was investigated in this paper. The controller was implemented using a moving base, and the beam model was an undamped shear beam. The control law was established using the storage function in the design technique. The finite-gain L_2 - stability of the feedback control system was then proven. This method dealt directly with the PDE of the beam model with no model reduction. Because of the non-collocated measurement and actuation in many applications, the backstepping observer was required for state estimation. Since the controller was implemented at the end of the beam via a moving base, the beam domain remained intact. Therefore, the method is simple to apply in applications. With the use of the finite-difference approach, the PDEs were numerically solved. The controller's performance of the proposed control scheme was demonstrated using computer simulation.

1. Introduction

Vibration suppressions of flexible beams are significant problems for applications such as robotics, space structures, flexible marine risers, etc. Beam models are infinite-dimensional or distributed-parameters systems in nature, so the equations of motion will be modeled using the partial differential equation (PDE). The state variables of a system depend on spatial and temporal variables.

The flexible beams' weight is less, so it consumes less energy but shows elastic vibration. When the robotic arm moves at high speed, vibration is unavoidable. As a result, the robotic arm has to slow down or even wait until the vibration dies down in many situations. This situation is time-consuming and counterproductive.

Boundary control has drawn much interest in the flexible beam vibration suppression field. However, a few sensors and actuators are needed for the control strategy. Control spillover is eliminated since the distributed parameter model is employed, i.e., no model reduction.

The undamped shear beam is examined in this work. This form of the beam can be used to model slender beams in applications. The most basic beam model is the Euler-Bernoulli beam. This beam model transforms into a shear beam when a shear deformation is included. Although the shear and Rayleigh beams are physically distinct, they are mathematically equivalent. The rotational inertia

* Corresponding author.
E-mail address: nipon413@hotmail.com (N. Boonkumkrong).

https://doi.org/10.1016/j.heliyon.2022.e12740
Received 3 February 2022; Received in revised form 15 December 2022; Accepted 22 December 2022
Available online 30 December 2022

Nomenclature

b	= positive constant
c_0	= spring constants
c_1	= damping constants
$\widetilde{c}_0$	= positive constant for an observer
m	= mass
i,j	= indexing superscripts and subscripts
I,J	= maximum index
$p\ (x,y)$	= observer gain kernel
q	$= r^2\ /\sqrt{\varepsilon}$
r	$= \Delta\ t\ /\Delta\ x$
s	$= \Delta\ t^2/\varepsilon$
t	= temporal variable
$\Delta\ t$	= temporal increment
$U(t)$	= controller
V	= storage function
$w\ (x,t)$	= beam displacement
$\widehat{w}\ (x,t)$	= estimation of $w\ (x,t)$
$\widetilde{w}\ (x,t)$	= observation error
$W\ (t)$	= displacement of a moving base
x,y	= spatial variables
$\overline{y},y^{'}$	= output
$\Delta\ x,\Delta\ y$	= spatial increment
X,Y	= Cartesian coordinate
ε,δ	= positive constant
ξ	= integration variable
φ	= rotation angle
φ	= any function
τ	= time
$\upsilon\ (t)$	= additional controller
$\widetilde{\upsilon}\ (x,t)$	= state variable of the target system
$\|w\|_2$	= Euclidean norm or L_2 – norm

term is incorporated in the Rayleigh beam model since it has a large cross-section area. Timoshenko beam is the most completed beam model incorporating all properties of beams. Derivations of beam models can be found in Han et al. [1].

Lasiecka presented the brief historical development of point and boundary controls for PDE-modeled systems [2]. The review paper summarizes the existing literature on distributed parameter systems found in Padhi et al. [3].

In the paper of Luo et al. [29] the shear force was applied to dampen rotational-joint robot vibration. The simple PI plus shear force feedback provided satisfactory control results.

Krstic et al. [4] introduced a new technique called backstepping boundary control for the engineering beams, such as the shear and Timoshenko beams, etc. This method combined the traditional damping boundary feedback control with the backstepping control concept. A coordinate transformation integral was used to transform the beam system into a stable wave equation with boundary damping. This approach was also adapted to use for the observer design. The well-posedness and stability were proved.

In 2014, the backstepping boundary control developed by Krstic et al. was used by Boonkumkrong et al. to control the rod temperature [5]. In 2018, Boonkumkrong et al. also implemented this control scheme to eliminate the vibration of the flexible beam mounted on the moving base [6].

Lertphinyovong and Khovidhungi [7] applied the backstepping boundary control technique to the Rayleigh beam.

In his paper, Morgul [8] studied clamped-free Euler-Bernoulli beams. The control force and torque were implemented at a free end. The Lyapunov function was used for proving. The vibration was suppressed uniformly and exponentially to zero.

Smyshlyaev et al. [9] investigated how the Euler-Bernoulli beam was controlled on its boundary. Position and moment actuators were implemented on one end, while the opposite end was the sliding boundary. The beam model was first expressed as the Schrödinger equation before using the backstepping technique in the design.

The control of the flexible beam's vibration was studied by Guo et al. [10]. After the beam system was re-expressed as a heat-like system, it was transformed into a target system using a backstepping technique. The original beam system was exponentially stable.

The stabilization of a shear beam rotating in the horizontal plane was studied by Dogan et al. [11]. The coordinate transformation with the backstepping technique was used to design the controller and observer. This technique was formally developed by Krstic et al. [4]. The proposed feedback control law achieved both a set-point regulation and vibration suppression. The results were satisfactory.

He and his colleagues examined the flexible maritime riser's vibration boundary control [12]. The analysis also took the vessel

model into account. Using Lyapunov's direct technique, the stability of the control scheme was proved. In the case of Zhao et al. [13], the riser displacement was decreased by the online control law. Investigations into the dead zone and saturation nonlinearities were also conducted.

He et al. studied how to control the vibration of a Timoshenko beam with spatiotemporal disturbance [14]. For controller design, Lyapunov's direct method was employed. The boundary observer was designed to account for the disturbance.

A tutorial presentation of a control design based on energy consideration was given by Ortega et al. [15]. Passivity and energy shaping concepts were presented. Matsuno et al. [16] considered the passivity of flexible mechanical systems. The Lyapunov function was introduced, and the controller was then derived. The controller was the PD and strain control law. The invariance principle and the differential operator were used for asymptotic stability proving.

The passivity-based control problem of the flexible beam was examined by Fard [17]. The controller was applied at the beam end. Semi-group and operator theories were used to prove the stability. The observer was not necessary and the control spillover was avoided because the beam model was not truncated.

The Timoshenko beam was investigated by Sasaki et al. [18]. The controller's design was based on the beam's passivity. Both translational and rotational beams were studied. The neural network was also used for gain tuning.

Zhao and Liu developed a disturbance rejection control for a Timoshenko manipulator exposed to disturbances [19]. The disturbance estimation error converged to zero in a finite time.

A flexible aerial refueling hose's boundary control was investigated by Liu et al. [20]. The boundary controller was designed using the backstepping method. Additionally, the control performance of the proposed approach and the conventional PD control were compared.

The spacecraft's flexible appendage with external disturbance was considered by Liu et al. [21]. The observer-based control scheme suppressed the vibration and tracked the desired attitude. An disturbance observer addressed the disturbance. It was also proven that the controlled system was stable.

Liu et al. [22] studied an unmanned spacecraft's vibration suppression and angle regulation. The adaptive NN control was designed. The modified barrier Lyapunov's direct method was used to ensure the angle tracking error in the limit.

Liu et al. [23] developed the boundary controllers for angle tracking and deformation suppression of a flexible variable-length rotary crane arm. An observer was used to deal with unknown extraneous disturbances. The auxiliary systems were used to deal with the asymmetric input saturations, and an asymmetric barrier Lyapunov function was used to verify the asymmetric output constraint.

The observer-based boundary control was applied to a flexible robotic manipulator by Liu et al. [24]. The disturbance observer's function was used to control the arm's position and dampen vibration. The stability and the well-posedness were shown.

Boonkumkrong et al. applied the boundary controller with a sliding base for vibration control of the shear beam. The effects of the parameter change of both the system and the controller on the control performance were studied [25].

In this paper, we investigate the suppression of the undamped shear beam vibrations. A passivity-based controller will be developed using the energy approach. The control design employs the beam's passivity property. The beam's energy function is chosen as a storage function and used to determine the control law. The designed controller is implemented by applying a shear force at the beam end. In this design approach, we deal with the PDE of the system directly. Model approximation or reduction is unnecessary; any term in the model is not truncated, so there is no control spillover problem. In the case of a non-collocated setup, the sensing and actuation are placed at the opposite boundaries, so a state estimation is needed. In this paper, we choose the backstepping observer for the state estimation.

This paper's main contributions include the following: (1) This technique incorporates the energy perspective for the controller design using the passivity property of the beam, (2) the sensing and the actuation configuration are non-collocated, and through the moving base, it is readily implementable in practical applications, and (3) the original PDEs are deal directly without model reduction.

The rest of the paper is arranged as follows. The mathematical model of the shear beam with the moving base and boundary conditions are introduced in Section 2. Sections 3 and 4 discuss passivity-based controller design and the backstepping observer. Sections 5 and 6 deal with numerical computations, simulation results, and related discussion. The paper's conclusion is displayed in Section 7. The proof for L_2 - stability is provided in AppendixA. Finally, the partial integrodifferential equation for the shear beam is derived in AppendixB.

2. Mathematical model

In this paper, the undamped shear beam will be used for the study. This kind of beam can be represented in many forms. In our controller design, the beam will be expressed as a coupled wave equation (1) and an ordinary differential equation (2) [18] as follows,

$$\varepsilon\ [w_{t\,t}(x,t) + W_{t\,t}\ (t)] = w_{xx}(x,t) - \varphi_x(x,t), \tag{1}$$

$$\varepsilon\,\varphi_{xx}(x,t) - \varphi\ (x,t) + w_x(x,t) = 0, \tag{2}$$

where the subscripts x and t represent the derivatives with respect to space and time, respectively, $w\ (x,t)$ is the beam displacement,x is the space along the beam,$W(t)$ is the displacement of the moving base,$\varepsilon > 0$ is a positive constant dependent on the beam's shear property, and φ is the rotational angle induced by the bending only.

The cantilevered shear beam model is depicted in Fig. 1. The beam is free at the left end and attached to the moving base at the right

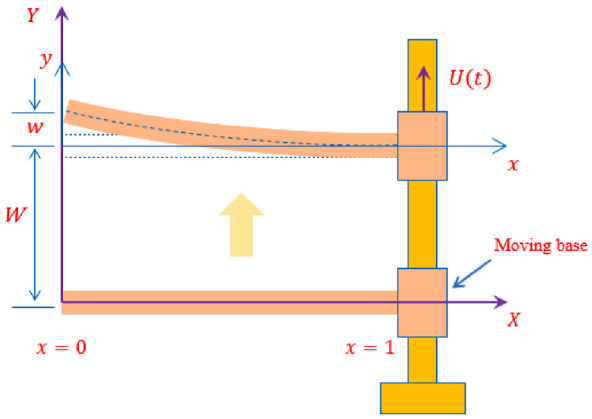

Fig. 1. Shear beam model with a moving base.

[25].

The effect of gravitational force is neglected due to the beam starting to move from its equilibrium position.

From Newton's second law, the equation of motion of the moving base is expressed as follows,

$$mW_{t\,t}(t) + [w_x(1,t) - \varphi\ (1,t)] = U(t) \tag{3}$$

where $U(t)$ is the passivity-based controller implemented at the base, and m is the mass of the moving base. The first term of (3) is the base's inertia force, and the second term is the force acting on the base due to the beam.

The following boundary conditions (4)–(7) are to be applied to the solution of (1) and (2) [26]:

$$w_x(0,t) - \varphi\ (0,t) = 0, \tag{4}$$

$$\varphi_x\ (0,t) = 0 \tag{5}$$

$$w\ (1,t) = 0, \tag{6}$$

$$\varphi\ \ (1,t) = 0. \tag{7}$$

At the free end on the left, there are no shear force (4) and no bending moment (5). And at the right end fixed to the base, there is no displacement (6) related to the base, and the slope (7) is zero.

3. Passivity-based boundary control

This section will design the boundary controller using the beam's passivity property. The control purpose is to eliminate the vibrating energy of the beam. To stabilize the system given by (1)–(2), which is subjected to the boundary conditions (4)–(7), the following controller (8) is proposed,

$$U\ (t) = -c_1\ W_t(t) + \upsilon\ (t), c_1 > 0, \tag{8}$$

where c_1 is the positive constant and $\upsilon\ (t)$ is an additional control element that needs to be identified. Notice that the first term on the right-hand side of (8) is a damping.

The displacement $w\ (x,t)$ will be written as w omitting the independent variables unless required. The storage function, V is defined in (9) as follows [25],

$$V = \frac{\varepsilon}{2}\int_0^1 [w_t + W_t]^2 dx + \frac{\varepsilon}{2}\int_0^1 {\varphi_x}^2 dx \tag{9}$$

$$+\frac{1}{2}\int_0^1 [\varphi - w_x]^2 dx + \frac{1}{2} m\ {W_t}^2.$$

Indeed, equation (9) is the energy function of the beam system. The integral terms are the kinetic and potential (strain) energies stored in the beam. The final term is the moving base's kinetic energy.

The rate of change of the energy in the beam can be obtained by differentiating the storage function, V, with respect to time,

$$\dot{V} = \varepsilon \int_0^1 [w_t + W_t]\ [w_{t\,t} + W_{t\,t}]\ dx + \varepsilon \int_0^1 \varphi_x\ \varphi_{xt} dx \tag{10}$$

$$+\int_0^1 [\varphi - w_x]\ [\varphi_t - w_{x\,t}]\,dx + m\ W_t\ W_{t\,t}.$$

Substituting (1) into (10) to obtain

$$\dot{V} = \int_0^1 [w_t + W_t]\ [w_{xx} - \varphi_x]\ dx + \varepsilon \int_0^1 \varphi_x\ \varphi_{xt}\ dx \quad (11)$$

$$+\int_0^1 [\varphi - w_x]\ [\varphi_t - w_{x\,t}]\,dx + m\ W_t\ W_{t\,t}.$$

Multiplying the square brackets in (11) to yield,

$$\dot{V} = \int_0^1 w_t\ [w_{xx} - \varphi_x]\ dx + \int_0^1 W_t\ [w_{xx} - \varphi_x]\ dx \quad (12)$$

$$+\varepsilon \int_0^1 \varphi_x\ \varphi_{xt}\ dx + \int_0^1 \varphi_t\ [\varphi - w_x]\ dx - \int_0^1 w_{x\,t}\ [\varphi - w_x]\,dx$$

$$+mW_t\ W_{t\,t}.$$

Due to the boundary conditions (4) to (7) and the integration of the second, third, and fifth integrals, (12) becomes,

$$\dot{V} = \int_0^1 w_t\ [w_{xx} - \varphi_x]\ dx + W_t\ [w_x(1) - \varphi\ (1)] \quad (13)$$

$$-\varepsilon \int_0^1 \varphi_{xx}\ \varphi_{\,t}\ dx + \int_0^1 \varphi_{\,t}\ [\varphi - w_x]\ dx$$

$$+\int_0^1 w_t\ [\varphi_x - w_{xx}]\,dx + mW_tW_{tt}.$$

From (2), the second and the third integrals in (13) vanish. Re-arranging the last integral and cancelling with the first integral so (13) becomes

$$\dot{V} = W_t\ [w_x(1) - \varphi\ (1)] + m\ W_t\ W_{t\,t}. \quad (14)$$

Substituting (3) into (14)

$$\dot{V} = W_t\ [U(t) - m\ W_{t\,t}] + m\ W_t\ W_{t\,t} \quad (15)$$

$$= W_t\ U(t).$$

Substituting the controller (8) into (15), we get (16)

$$\dot{V} = W_t\ [-c_1\ W_t\ + \upsilon\ ]. \quad (16)$$

For passivity proving, we let $\overline{y} = W_t$ be an output, so (16) becomes (17) and then (18),

$$\dot{V} = \overline{y}(-c_1\overline{y} + \upsilon) \quad (17)$$

$$= \upsilon\overline{y} - c_1\overline{y}^2$$

$$\dot{V} \leq \upsilon\ \overline{y}. \quad (18)$$

3.1. Definition 1

If a storage function, V, a continuously differentiable positive semi-definite function, exists [27], then

$$\upsilon^T\overline{y} \geq \dot{V}, \quad (19)$$

From (19), the system is said to be passive, where υ and $\overline{y}$ represent the input and the output, respectively.

From definition 1, system (1) and (2) with the controller (8) is passive.

3.2. Lemma 1

The system is finite gain L_2-stable if the output is strictly passive with $v^T\bar{y} \geq \dot{V} + \delta\bar{y}^2$ for some $\delta > 0$ [27].

In AppendixA, the proof of Lemma 1 is shown.

Since system (1) and (2) with the controller (8) are output strictly passive, it follows from lemma 1 that the feedback control system is finite gain L_2 - stable.

Because the beam is fixed to the moving base, the controller (8) can now be expressed as,

$$U(t) = -c_t w_t\ (1,t) + v\ (t). \tag{20}$$

Using the state feedback control principle, the additional control input v can be chosen. We define state feedback variable as $y' = w\ (1,t)$. The system can be stabilized by the control $v = -\varphi\ (y')$ with any function φ such that $y'^T\varphi\ (y') > 0$ and $\varphi\ (0) = 0$ for all $y' \neq 0$, then we can select the following feedback control (21) as an additional control component,

$$v\ (t) = -c_0 w\ (1,t), c_0 > 0, \tag{21}$$

where c_0 is a positive constant.

Substituting (21) into (20), we obtain,

$$U(t) = -c_0 w\ (1,t) - c_1 w_t\ (1,t). \tag{22}$$

The feedback controller (22) is the passivity-based controller. The feedback variables are the displacement, $w\ (1,t)$, and its derivative, $w_t(1,t)$, at the beam's base.

In this case, the sensing and actuation are placed at the same location $(x = 1)$, so the state estimator is not required. The setup is collocated.

The terms in the controller are meaningful in a real problem and correspond to physical variables. The first term is the damping force used to damp out the vibration. The second term of the controller (22) is used to reshape the potential energy to $1/2c_0w^2$, which has a unique minimum at $w = 0$ [27]. The proposed passivity-based controller perform like a proportional-derivative (PD) controller. The control forces are exerted on the moving base via base movements.

4. Backstepping observer

In the last section, the beam setup is collocated i.e., the sensing and actuation are both located at the same boundary. For some control applications, it may be desired to change the setup to an anti-collocation, i.e., the sensing and actuation are located at opposite boundaries. This kind of setup makes the control readily implementable in practical applications. In this case, the sensor is moved to the left boundary, and the actuator or controller remains applied at the right end. For this situation, a state estimation or an observer is needed. The observer will use only measurements at the beam's tip for the state estimation.

In this paper, the so-called backstepping observer is employed for state estimation. This novel method was developed by Krstic et al. [4]. This kind of observer can be applied directly to the beam's PDE.

Another way to write the undamped shear beam is as follows:

$$\varepsilon\ w_{tt} = w_{xx} + b^2 w + b^3 \int_0^1 \sinh\ (b(x-y))\ \ w(y)\ \ dy \tag{23}$$

$$-b^2 \cosh\ (bx)\ \ w(0) - b \sinh\ (bx)\ \ \varphi(0),$$

$$w_x(0) = \varphi\ (0). \tag{24}$$

AppendixB illustrates how (23)–(24) was derived. As before, the displacement $w\ (x,t)$ will be written as w omitting the independent variables unless required.

The backstepping observer is given by the following PDE,

$$\varepsilon\ \widehat{w}_{tt} = \widehat{w}_{xx} + b^2\widehat{w} + b^3 \int_0^x \sinh\ (b\ (x-y))\ \ \widehat{w}(y)\ \ dy \tag{25}$$

$$-b^2 \cosh\ (b\ x)\ w\ \ (0) - b \sinh\ (b\ x)\ \varphi\ \ (0)$$

$$+p_y(x,0)\ \ (w\ (0) - \widehat{w}\ (0))$$

$$\widehat{w}_x\ (0) = \varphi\ \ (0) + p\ \ (0,0)\ (w\ (0) - \widehat{w}\ (0)) \tag{26}$$

$$-\widetilde{c}_0(w_t(0) - \widehat{w}_t(0)),$$

$$\widehat{w}\ \ (1) = w\ (1), \tag{27}$$

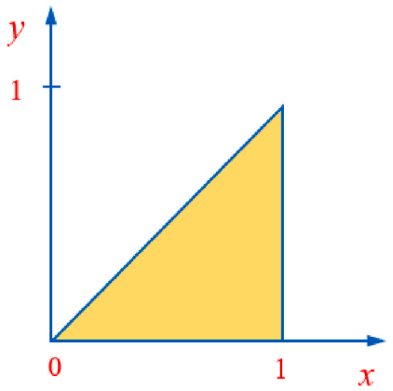

Fig. 2. Domain of the observer gain kernel PDE.

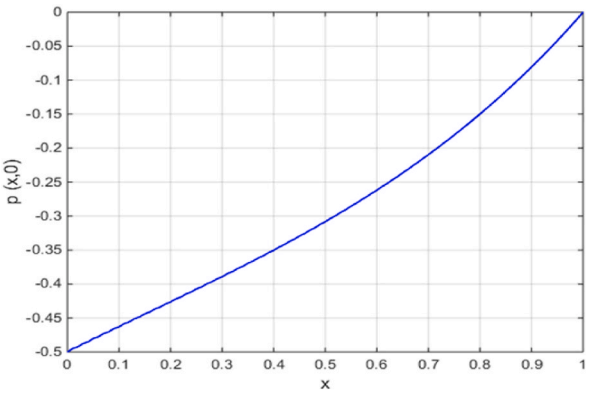

Fig. 3. The observer gain function, $p(x,0)$.

where $\widehat{w}$ is the estimation of w, $p\ (x,y)$ is an observer gain kernel,$\widetilde{c}_0$ is the positive constant, and$b\ = 1\ /\sqrt{\varepsilon}$. The observer employs the measurements of displacement $w\ (0,t)$ and angle $\varphi\ (0,t)$ at the beam's tip. Solving the PDEs (28)–(30) yields the observer gain kernels $p_y(x,0)$ and $p\ (0,0)$ used in (25)–(26), respectively,

$$p_{yy} = p_{xx} + b^2 p - b^3 \sinh(b(x-y)) \tag{28}$$

$$+b^3 \int_y^x p\ (\xi, y)\sinh\ (b(x-\xi))\ \ d\xi,$$

$$p\ (x,x) = \frac{b^2}{2}(x-1), \tag{29}$$

$$p\ (1,y) = 0. \tag{30}$$

This PDE, which has a lower triangle as its domain and is of the hyperbolic type, is shown in Fig. 2.
Subtracting (25)–(27) from (23)–(24) yielding the following observer error PDE,

$$\varepsilon\widetilde{w}_{tt} = \widetilde{w}_{xx} + b^2\widetilde{w} + b^3 \int_0^x \sinh(b\ (x-y))\ \ \widetilde{w}\ (y)\ \ dy. \tag{31}$$

$$+p_y(x,0)\ \ \widetilde{w}\ \ (0),$$

$$\widetilde{w}_x\ (0) = -\,p\ (0,0)\ \widetilde{w}\ (0) + \widetilde{c}_0\ \widetilde{w}_t(0), \tag{32}$$

$$\widetilde{w}\ \ (1) = 0. \tag{33}$$

where $\widetilde{w} = w - \widehat{w}$ is the observer error.
Using the following coordinate transformation

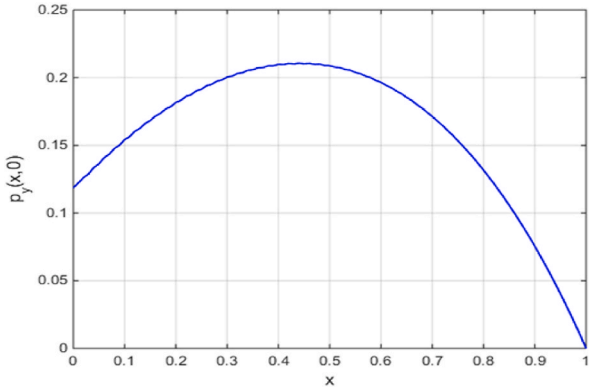

Fig. 4. The observer gain function, $p_y(x,0)$.

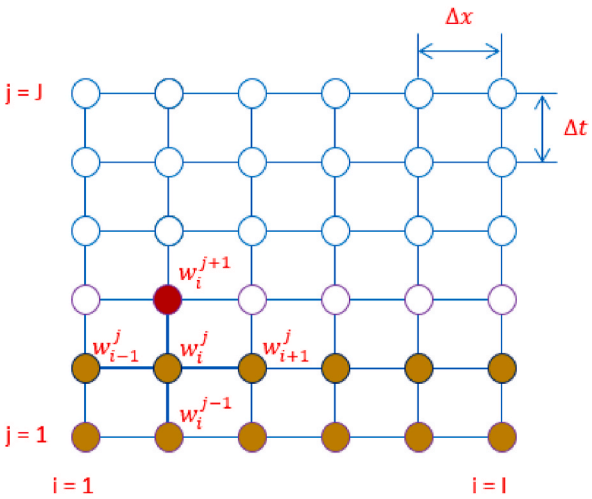

Fig. 5. Calculation grid for the beam.

$$\widetilde{w}(x) = \widetilde{\upsilon}\ (x) - \int_0^x p\ (x,y)\ \widetilde{\upsilon}(y)\ dy, (34)$$

to convert Eqs. (31–33) into the following target system,

$$\varepsilon\, \widetilde{\upsilon}_{tt} = \widetilde{\upsilon}_{xx}, (35)$$

$$\widetilde{\upsilon}_x(0) = \widetilde{c}_0\, \widetilde{\upsilon}_t(0), (36)$$

$$\widetilde{\upsilon}\ (1) = 0, (37)$$

where $\widetilde{\upsilon}$ is the state variable.

System (35)–(37) is known to be exponentially stable. From this transformation, the observer gain PDE (28)–(30) are obtained. The proof of the convergence of the observer can be found in the paper of Krstic et al. [4]. The observer gain kernels $p\ (x,0)$ and $p_y(x,0),$ are depicted in Figs. 3 and 4, respectively.

As shown by Krstic et al. [28], the variable, $w\ (1)$ in (27), can be set to zero or substituted with some other control policy, in our case, the passivity-based controller.

For the state estimation, the backstepping observer (25)–(27) with the observer gain kernel PDE (28)–(30) are used. In the case of the observer, the feedback variables $\widehat{w}\ \ (1,t)$, and $\widehat{w}_{\ t}\ (1,t)$ are used instead in the controller (38) as follows,

$$U(t) = -c_0\widehat{w}\ \ (1,t) - c_1\widehat{w}_t\ (1,t) \quad (38)$$

5. Numerical calculation

The finite difference (FD) method is used to compute the partial derivative and integral terms for the numerical simulation of the beam's dynamics. The first-order and the second-order difference equations are used to discretize the PDE's derivative terms. The integral term can be calculated using the trapezoidal integration rule. The calculation grid is shown in Fig. 5, where Δx is the spatial increment and Δt is the time increment, which are indexed by i and j, respectively.

The finite difference equations can be used to express the beam model (23) as follows:

$$w_i^{j+1} = \left(2 - 2q + s\,b^2\right) w_i^j - w_i^{j-1} + q\left(w_{i+1}^j + w_{i-1}^j\right)$$

$$+s\,b^3\Delta y \begin{pmatrix} 0.5\sinh\left(b\left(x_i - y_1\right)\right) w_1^j \\ \sum_{k=2}^{i-1} \sinh\left(b\left(x_i - y_k\right)\right) w_k^j \\ 0.5\sinh\left(b\left(x_i - y_i\right)\right) w_i^j \end{pmatrix}$$

$$-s\,b^2\cosh\left(b\,x_i\right) w_1^j - \frac{s\,b}{\Delta x}\sinh\left(b\,x_i\right)\left(w_2^j - w_1^j\right) \tag{39}$$

where $r = \Delta t/\Delta x, q = r^2/\varepsilon$ and $s = (\Delta t)^2/\varepsilon$.

Fig. 5 shows the grid nodes or elements of the first and the second rows (colored elements) calculated using the initial conditions. The elements w_i^{j+1} in each row are calculated from $i = 2$ to $i = I - 1$ by using the information from the previous two rows.

For the first element w_1^{j+1} at $x = 0$, equations (24), (B5) from AppendixB and (7) are employed to get (40) as follows,

$$w_1^{j+1} = \tag{40}$$

$$\frac{b^2(\Delta x)^2}{\cosh(b)\left(b\,\Delta x\tanh(b) - \frac{0.5\,b^2(\Delta x)^2}{\cosh(b)}\cosh\left(b\left(1 - y_1\right) - 1\right)\right)}$$

$$\times \begin{pmatrix} \sum_{k=2}^{I-1} \cosh\left(b\left(1 - y_k\right)\right) w_k^{j+1} \\ +0.5\cosh\left(b\left(1 - y_I\right)\right) w_I^{j+1} \end{pmatrix}$$

For the last element, w_I^{j+1} at $x = 1$, can be calculated from (3) and (22) to obtain (41) as follows,

$$w_I^{j+1} = \left(2 - \frac{(\Delta t)^2}{m\,\Delta x} - c_1\frac{\Delta t}{m} - c_0\frac{(\Delta t)^2}{m}\right) w_I^j \tag{41}$$

$$+\left(c_1\frac{\Delta t}{m} - 1\right) w_I^{j-1} + \frac{(\Delta t)^2}{m\,\Delta x} w_{I-1}^j.$$

For the observer, the calculation grid is the same as Fig. 5, but replaces the variable w_i^j with $\widehat{w}_i^j$. The finite difference equation of the observer (25) is the same as (39) and there is a term $s\,p_{y_i}^1(w_1^j - \widehat{w}_1^j)$ added.

The first element (26) of the observer was expressed by (42) as follows,

$$\widehat{w}_1^{j+1} = \frac{1}{\left(1 - \Delta x\,p_1^1 + \frac{\widetilde{c_0}}{r}\right)} \tag{42}$$

$$\times\left\{\ \widehat{w}_2^{j+1} - w_2^{j+1} + \left(1 - \Delta x\,p_1^1\right) w_1^{j+1}\right.$$

$$\left.+\frac{\widetilde{c_0}}{r}\left(w_1^{j+1} - w_1^j + \widehat{w}_1^j\right)\right\}$$

The last element (27) was calculated from $\widehat{w}_I^{j+1} = w_I^{j+1}$

The observer gain kernel PDE, from (28) the elements p_i^{j-1} can be expressed by the following finite difference equations,

$$p_i^{j-1} = p_{i+1}^j + p_{i-1}^j - p_i^{j+1} + (\Delta x)^2 b^2 p_i^j$$

$$-(\Delta x)^2 b^3\sinh\left(b\left(x_i - y_j\right)\right)$$

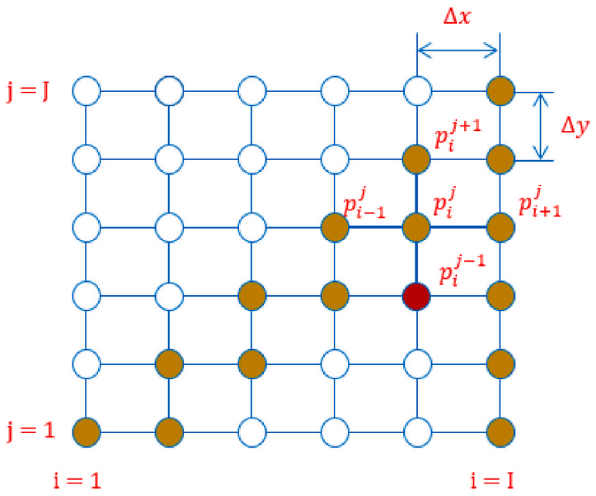

Fig. 6. Calculation grid for the observer kernel.

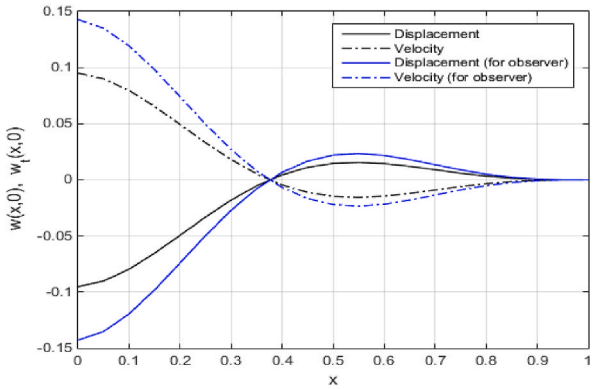

Fig. 7. Initial displacement and velocity at $t = 0$.

$$+(\Delta x)^3 b^3 \begin{pmatrix} 0.5\, p_j^j \sinh\left(b\left(x_i - y_j\right)\right) \\ \sum_{k=j+1}^{i-1} p_k^j \sinh\left(b\left(x_i - y_k\right)\right) \\ 0.5\, p_i^j \sinh\left(b\left(x_i - y_i\right)\right) \end{pmatrix}. \tag{43}$$

The computation domain is $0 \le y \le x \le 1$. The calculation grid with the spatial increments Δx and Δy is shown in Fig. 6. The diagonal and off-diagonal elements can be obtained from (29) and its derivative, respectively, and the last column can be calculated from (30).

The calculation using (43) is performed backward from $J-3$ and $I-1$ since the known information is first available from there.

6. Simulation result and discussion

This section presents the beam simulations with and without the observer cases. The finite difference equations from the previous section will be employed to solve the PDE.

The numerical simulations are performed using MATLAB code. Parameter values are $\varepsilon = 1, m = 0.05, c_0 = 1.0$, $c_1 = 1.75$ and $\widetilde{c}_0 = 0.75$. The time and space increments in the calculation are $\Delta t = 0.01$ and $\Delta x = 0.025$, respectively.

The following initial conditions are used to start the beam vibrating motion [4],

$$w(x,0) = 0.1\ (1-x)^2 \sin\left(1.6\,\pi\ (1-x)\right) \tag{44}$$

$$w_t(x,0) = -0.1\ (1-x)^2 \sin\left(1.6\,\pi\ (1-x)\right). \tag{45}$$

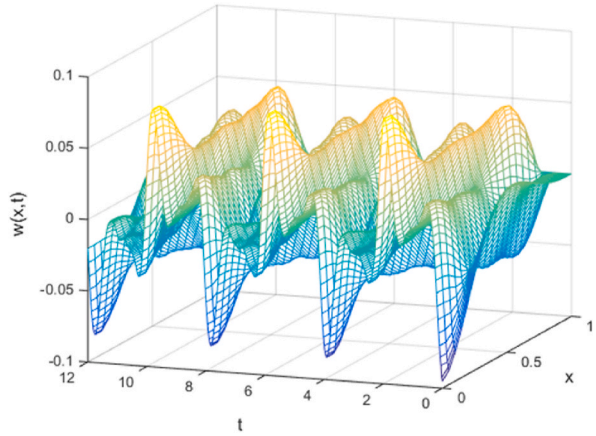

Fig. 8. Simulated beam without the controller.

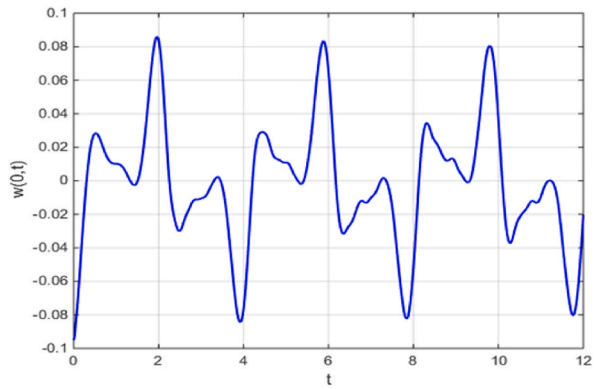

Fig. 9. Beam's tip displacement of the uncontrolled case.

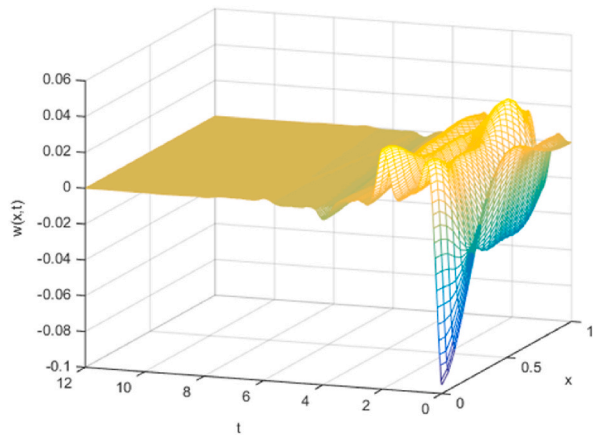

Fig. 10. Beam simulation with the controller.

Equations (44) and (45) represent the initial beam displacement and velocity, as shown in Fig. 7. For the observer, the initial conditions are increased by 50%.

For the uncontrolled case, the beam model with no controller was simulated with the initial conditions. The system energy was conserved since the beam model contains no damping term. Within the system, there are only energy transformations between potential and kinetic energies. Fig. 8 demonstrates that the response is oscillatory. Fig. 9 shows the displacement of the beam's tip.

Fig. 10 depicts the beam simulation with the controller applied at the moving base. In this case, the controller's damping

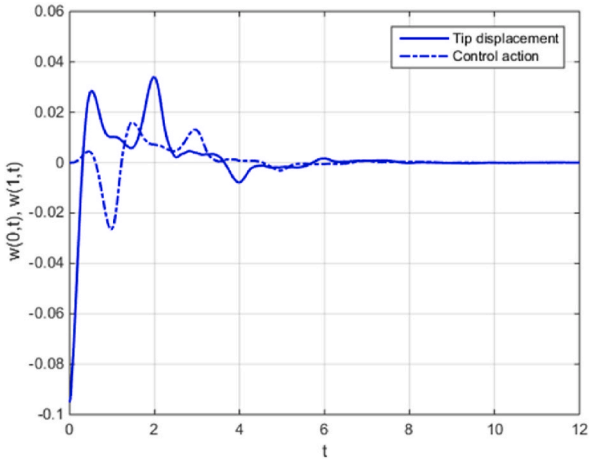

Fig. 11. Tip displacement and control action.

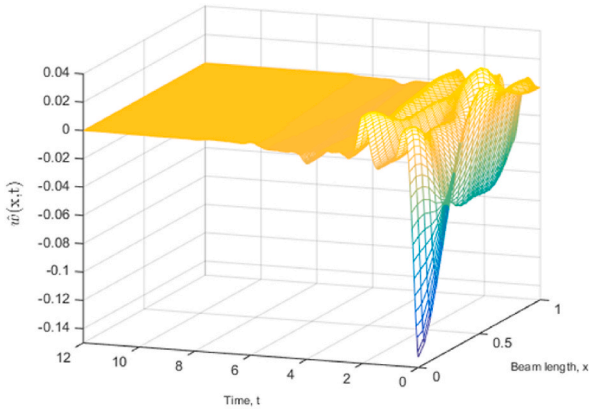

Fig. 12. Beam simulation with the observer.

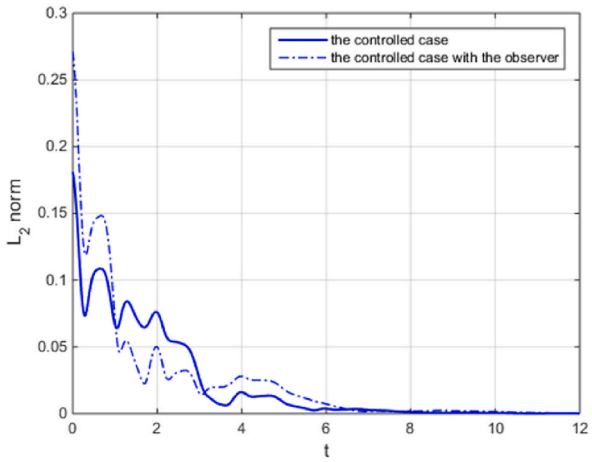

Fig. 13. L_2 norms of the system with/without the observer.

component, $-c_1 w_t\ (1,t)$ dissipated the beam's vibrating energy. Finally, the beam reached its equilibrium through the elastic component, $-\ c_0 w\ (1,t)$. Fig. 11 shows the tip displacement of the beam compared to the control action at the opposite end. The feedback system was stabilized in the sense of L_2 - stability. For the control scheme proposed by Sasaki, the neural network algorithm is

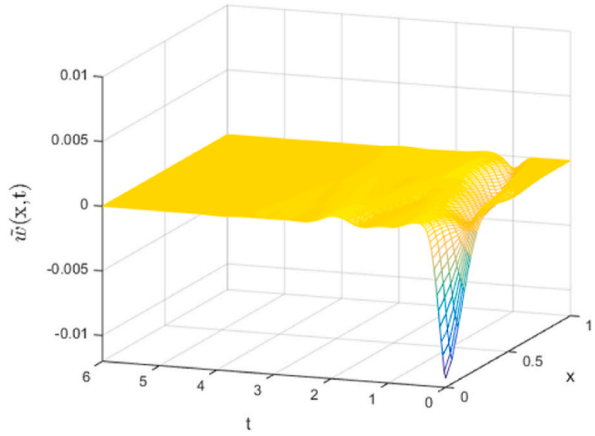

Fig. 14. The observer error.

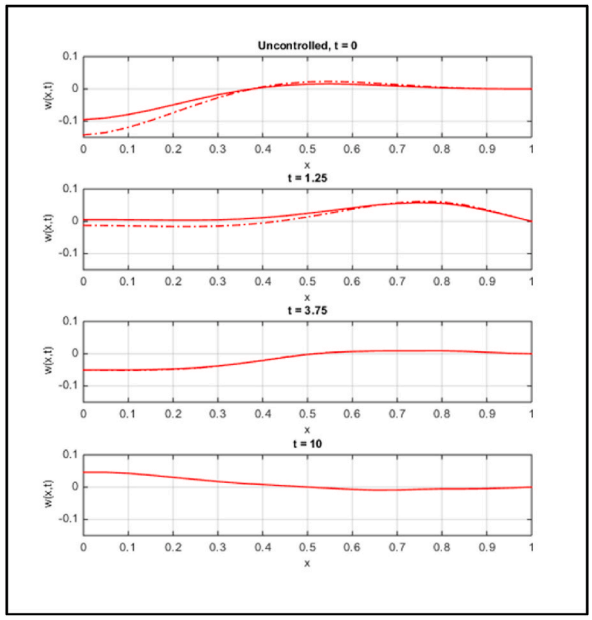

Fig. 15. Snapshots of the uncontrolled beam.

needed for parameter tuning so that the response can reach equilibrium [18].

The simulation result of the beam model with the observer (25)–(27) is shown in Fig. 12. The observer used the feedback from the measurements at the beam's tip, i.e., the tip displacement, $w(0,t)$ and the tip velocity, $w_t(0,t)$. Note that the system with observer began to vibrate from the initial conditions, which were 50% greater than the system without the observer. The beam was also L_2 -stabilized.

The L_2 norm, or the Euclidean norm, as expressed in Eq. (46), is used to measure the energy level that remains in the system [27].

$$\|w\|_2 = \sqrt{|w_1|^2 + \cdots + |w_I|^2} \tag{46}$$

The settling time is used to measure how fast the response is to settle down. It is the time taken by the beam's L_2 norm to be within 2% of the maximum L_2 norm of the initial conditions. Fig. 13 shows the L_2 norms of the system with and without the observer.

For the system without the observer, the settling time was at $t = 6.42$, and for the system with the observer, it was at $t = 5.07$.

The observer error is shown in Fig. 14. The observer error response decreases to zero as $t \to \infty$.

Fig. 15 shows the snapshots of the uncontrolled beam in the sequences of time both without and with the observer. The beams in both cases coincided after $t = 3.75$. The beam was endlessly vibrating since there was no damping to drive out the vibration.

The controlled beam snapshots are displayed in Fig. 16. The responses settled down to equilibrium with the controller in action.

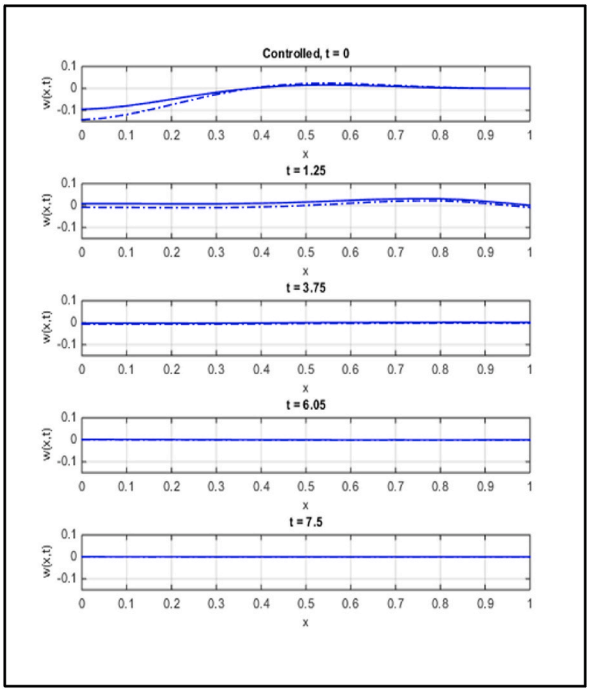

Fig. 16. Snapshots of the controlled beam.

7. Conclusion

The investigation on flexible beam vibration control was carried out in this research. The control scheme was designed on the concept of energy. This method allows us to deal with the system's PDEs directly. Furthermore, the control spillover was avoided since the beam model was not truncated. The system's energy function was defined as the storage function and then employed in controller design. The proposed controller had the dynamics of the damper-spring mechanism. The feedback control system's finite gain L_2 - stability has been proved. Since, for the practical applications, the actuation and the sensing were non-collocated, then the back-stepping observer was needed for state estimation. With the use of the finite difference approach, the PDEs were numerically solved. The simulation results for the beam controls were shown, both with and without the observer. The controller is simple and effective in eliminating the vibrating energy of the beam. For further research, the external loading and the disturbance will be included in the controller design.

Acknowledgments

The authors appreciate Srinakharinwirot University and King Mongkut's University of Technology, North Bangkok, for all their support and cooperation on this research.

Appendix A

The proof of Lemma 1

Let V be a storage function, and its time derivative satisfies the following inequality [27]:

$$\dot{V} \leq \upsilon^{T}\overline{y} - \delta\,\overline{y}^{T}\overline{y} = -\frac{1}{2\delta}(\upsilon - \delta\,\overline{y})^{T}(\upsilon - \delta\,\overline{y}) \quad (A\ 1)$$

$$+\frac{1}{2\delta}\upsilon^{T}\upsilon - \frac{\delta}{2}\overline{y}^{T}\overline{y}$$

$$\leq \frac{1}{2\delta}\upsilon^{T}\upsilon - \frac{\delta}{2}\overline{y}^{T}\overline{y}.$$

Integrating both sides of the inequality over $[0, \tau]$, yielding

$$\int_0^\tau \bar{y}^T(t)\,\bar{y}\ (t)\ dt \le \frac{1}{\delta^2}\int_0^\tau v^T(t)\,v\ (t)\ dt - \frac{2}{\delta}\int_0^\tau \dot{V}\ dt.$$

$$\le \frac{1}{\delta^2}\int_0^\tau v^T(t)\,v\ (t)\ dt$$

$$-\frac{2}{\delta}\ [V(w\ (\tau)) - V(w\ (0))].$$

For non-negative numbers a and b, the inequalities $V \ge 0$ and $\sqrt{a^2+b^2} \le a+b,$ hold, so we get

$$\|\bar{y}_\tau\|_{L_2} \le \frac{1}{\delta}\|v_\tau\|_{L_2} + \sqrt{\frac{2}{\delta}V(w\ (0))}, (A2)$$

where $\|\bar{y}_\tau\|_{L_2}$ and $\|v_\tau\|_{L_2}$ areL_2- norms of the input and the output, respectively. So, this proves the lemma.

Appendix B

The partial integrodifferential equations of the shear beam.
The undamped shear beam model in the local coordinate $x-y$ can be expressed as [4],

$$\varepsilon\, w_{t\,t}(x,t) = w_{xx}(x,t) - \varphi_x(x,t), (B\ 1)$$

$$\varepsilon\, \varphi_{xx}(x,t) - \varphi(x,t) + w_x(x,t) = 0. \quad (B2)$$

Using Laplace transform to solve the ODE (B2) in x, yielding

$$\varphi\ (x) = \cosh(b\,x)\ \varphi\ (0) \quad (B\ 3)$$

$$-b\int_0^x \sinh(b\,(x-y))\, w_y(y)\ dy.$$

Performing integration to the integral term in (B3) to obtain,

$$\varphi\ (x) = \cosh(b\,x)\ \varphi\ (0) + b\sinh(b\,x)\, w(0) \quad (B\ 4)$$

$$-b^2\int_0^x \cosh(b\,(x-y))\, w\ (y)\ dy.$$

Solving (B4) for $\varphi\ (0)$ by setting $x = 1$,

$$\varphi\ (0) = \frac{1}{\cosh(b)}\ \left[\varphi(1) - b\sinh(bx)\, w(0) \quad (B\ 5)\right.$$

$$\left.+b^2\int_0^1 \cosh(b\,(1-y))\, w\ (y)\ dy\right].$$

Substituting $\varphi\ (0)$ into (B4), we get

$$\varphi\ (0) = \frac{\cosh(b\,x)}{\cosh(b)}\ \left[\varphi(1) - b\sinh(b)\, w(0) \quad (B6)\right.$$

$$\left.+b^2\int_0^1 \cosh(b\,(1-y))\, w\ (y)\ dy\right]$$

$$+b\sinh(b\,x)\, w(0) - b^2\int_0^1 \cosh(b\,(x-y))\, w\ (y)\ dy.$$

To obtain (23), we differentiate (B6) with respect to x to get $\varphi_x\ (x,t)$ and put it into (B1). From the boundary condition (4), we get (24).

References

[1] S.M. Han, H. Benaroya, T. Wei, Dynamics of Transversely vibrating beams using four engineering theories, J. Sound Vib. 225 (5) (1999) 935–998.

[2] I. Lasiecka, Control of Systems Governed by Partial Differential Equation Paper Presented at the the Proceedings of the 34th Conference on Decision & Control, 1995 (New Orleans, LA).
[3] R. Padhi, S.F. Ali, An account of chronological developments in control of distributed parameter systems, Annu. Rev. Control 33 (2009) 59–68.
[4] M. Krstic, B.-Z. Guo, A. Balogh, A. Smyshlyaev, Control of a tip-force destabilized shear beam by observer-based boundary feedback, SIAM J. Control Optim. 47 (2) (2008).
[5] N. Boonkumkrong, S. Kuntanapreeda, Backstepping boundary control: an application to rod temperature control with Neumann boundary condition, Journal of Systems and Control Engineering 228 (5) (2014) 295–302.
[6] N. Boonkumkrong, S. Chinvorarat, P. Asadamongkon, Backstepping boundary control: an application to the suppression of flexible beam vibration, IOP Conf. Ser. Mater. Sci. Eng. (2018). Paper presented at the the IOP Conference Series: Materials Science and Engineering, 297(1), 1-11.
[7] J. Lertphinyovong, W. Khovidhungij, Backstepping Boundary Controllers and Observers for the Rayleigh Beam Paper Presented at the Proceedings of the 17th World Congress, The international federation of automatic control, Seoul Korea, 2008.
[8] O. Morgul, Dynamic boundary control of the Timoshenko beam, automatica, Automatica 28 (6) (1992) 1255–1260.
[9] A. Smyshlyaev, B.-Z. Guo, M. Krstic, Arbitrary decay rate for Euler-Bernoulli beam by backstepping boundary feedback, IEEE Trans. Automat. Control 54 (5) (2009).
[10] B.-Z. Guo, F.F. Jin, Backstepping approach to the arbitrary decay rate for Euler–Bernoulli beam under boundary feedback, Int. J. Control 83 (10) (2010) 2098–2106.
[11] M. Dogan, O. Morgul, Boundary control of a rotating shear beam with observer feedback, J. Vib. Control 18 (14) (2011) 2257–2265.
[12] W. He, B.V.E. How, S.S. Ge, Y.S. Choo, Boundary Control of a Flexible Marine Riser with Vessel Dynamics, Marriott Waterfront, Baltimore, MD, USA, 2010. Paper presented at the 2010 American control conference.
[13] Z. Zhao, X. He, Z. Ren, G. Wen, Boundary adaptive robust control of a Flexible riser system with Input Nonlinearities, IEEE Transactions on Systems, Man , and Cybernetics system 49 (10) (2019).
[14] W. He, S. Zhang, S.S. Ge, Boundary output-feedback stabilization of a Timoshenko beam using disturbance observer, IEEE Trans. Ind. Electron. 60 (11) (2013).
[15] R. Ortega, A.J.v. d. Schaft, I. Mareels, B. Maschke, *Energy Shaping Revisited* Paper Presented at the Proceedings of the 2000 IEEE International Conference on Control Applications, September 25-27, Anchorage, Alaska, USA, 2000.
[16] F. Matsuno, K. Murata, Passivity And PDS Control of Flexible Mechanical Systems on the Basis of Distributed Parameter System Paper Presented at the IEEE International Conference on Systems, Man, and Cybernetics, Tokyo, Japan, 1999.
[17] M.P. Fard, Passivity analysis of nonlinear Euler-Bernoulli beams, Model. Ident. Control 23 (4) (2002) 239–258.
[18] M. Sasaki, T. Shimizu, Y. Inoue, W.J. Book, Self-Tuning Vibration Control of a Rotational Flexible Timoshenko Arm Using Neural Networks. Advances in Acoustics and Vibration, 2012.
[19] Z. Zhao, Z. Liu, Finite-time convergence disturbance rejection control for a flexible Timoshenko manipulator, IEEE/CAA Journal of Automatica Sinica 8 (1) (2021).
[20] Z. Liu, J. Liu, W. He, Modeling and vibration control of a flexible aerial refueling hose with variable lengths and input constraint, Automatica 77 (2017) 302–310.
[21] Y. Liu, Y. Fu, W. He, Q. Hui, Modeling and observer-based vibration control of a flexible spacecraft with external disturbances, IEEE Trans. Ind. Electron. 66 (11) (2018) 8648–8658.
[22] Y. Liu, X. Chen, Y. Wu, H. Cai, H. Yokoi, Adaptive neural network control of a flexible spacecraft subject to input nonlinearity and asymmetric output constraint, IEEE Transact. Neural Networks Learn. Syst. (2021) 1–9.
[23] Y. Liu, Y. Mei, H. Cai, C. He, T. Liu, G. Hu, Asymmetric input–output constraint control of a flexible variable-length rotary crane arm, IEEE Trans. Cybern. (2021) 1–10.
[24] Y. Liu, X. Chen, Y. Mei, Y. Wu, Observer-based Boundary Control for an Asymmetric Output-Constrained Flexible Robotic Manipulator, vol. 65, Science Chian Information Sciences, 2022.
[25] N. Boonkumkrong, S. Chinvorarat, P. Asadamongkon, Passivity-based boundary control for vibration suppression of the shear beam, Adv. Mech. Eng. 14 (11) (2022) 1–11.
[26] S.S. Rao, Mechanical Vibration, 3 ed., Addison-Wesley Publishing Company, 1995.
[27] H.K. Khalil, Nonlinear Systems, 3 ed., Prentice-Hall, 2002.
[28] Krstic M., Siranosian A.A., Smyshlyaev A., Backstepping Boundary Controllers and Observers for the Slender Timoshenko Beam: Part I – Design. Paper Presented at the Proceedings of the 2006 American Control Conference, Minneapolis, Minesota, USA, 2006, June, 2412-2417.
[29] Z.H. Luo, N. Kitamura, B.Z. Guo, Shear force feedback control of flexible robot arms, IEEE Transactions on Robotics and Automation 11 (5) (1995) 760–765.